Western States Section/The Combustion Institute/1997 Fall Meeting

NITROUS OXIDE CONSUMPTION AND FLAMMABILITY LIMITS OF H_2–N_2O–AIR AND CH_4–N_2O–O_2–N_2 MIXTURES

U. PFAHL AND J.E. SHEPHERD

Graduate Aeronautical Laboratories
California Institute of Technology
Pasadena, CA 91125, USA

Explosion Dynamics Laboratory Report FM97-16

Abstract

The nitrous oxide consumption during combustion of different fuel-oxidizer mixtures was investigated experimentally. Experiments were carried out in an 11.25-liter combustion vessel at initial pressures of 100 kPa. The examined mixtures were hydrogen-nitrous oxide-air and methane-nitrous oxide-air (10 volume % N_2O). Pre- and post-burn gas-analysis of reactants and products were done for hydrogen, methane, nitrous oxide, oxygen and nitrogen by using gas chromatography and Fourier transform infrared spectrometry.

Furthermore, lower and upper flammability limits of methane-nitrous oxide mixtures at initial pressures of 100 kPa have been determined. The influence of nitrogen dilution up to the inerting concentration, of small amounts of oxygen and of variation of the ignition energy on the flammability limits has been investigated in this study as well.

The behavior of nitrous oxide consumption in hydrogen-nitrous oxide-air mixtures is very different than in methane-nitrous oxide-air mixtures. Whereas the nitrous oxide completely dissociates during combustion of all flammable methane-nitrous oxide-air mixtures it only partially dissociates for lean hydrogen-nitrous oxide-air mixtures (less than 14% H_2). For barely flammable hydrogen-nitrous oxide-air mixtures (6% H_2), almost no nitrous oxide is consumed. There is a distinct increase in the nitrous oxide consumption as the initial hydrogen concentration is increased from 8% to 9%.

The lower flammability limit of methane-nitrous oxide mixtures occurs at 2.7% methane for ignition energies less than 10 Joules. This value increases to 4.7% for ignition energies less than 0.04 Joule. The upper flammability limit is between 40 and 50% methane for ignition energies less than 10 Joules. Addition of 70% N_2 will inert the mixture. Small amounts of oxygen (3 - 5 volume %) do not significantly influence the limits or inerting condition.

1 Introduction

Much information is available on the combustion process of fuel-oxidizer mixtures using air or oxygen as oxidants, but there is little information available on using nitrous oxide as oxidizer or as one component of a combustible gas mixture. It was noticed in early studies, that the behavior of N_2O during combustion varies greatly [1]. Depending on mixture composition, ignition energy and explosion temperature, the nitrous oxide can behave as a diluent, or an oxidizer, or it can exothermically dissociate to act as an explosive. The standard heat of reaction $\Delta_R H^\circ$ for the nitrous oxide dissociation $N_2O \longrightarrow N_2 + 1/2\ O_2$ amounts to -82.1 kJ/mol.

Flammability of the individual fuels (hydrogen and methane) in air is well characterized [14]. Available data on limits is summarized in Table 1. However, there are some peculiar aspects to these fuel-oxidizer combinations, particularly with mixtures containing N_2O. Nitrous oxide decomposes slowly at low temperatures but is extremely exothermic. N_2O can behave as an explosive if the ignition stimulus is large enough and there are sufficient H atoms present to catalyze the decomposition [15]. However, for very low temperature flames, the N_2O does not appear to react at all. H_2 has a very large flammability range and unusually high flame speeds. Flammability of fuels in N_2O is not as well characterized as in air. At the time we started this study, no information was available on CH_4 limits. Our present data on the limits are given in Table 2.

Fuel	LFL		ST	UFL	Inert (N_2)
	UPL	DPL			
H_2	4	8	29.6	75	70
CH_4	5		9.5	15	37

Table 1: Flammability limits for fuel-air mixtures at NTP. Amounts are given in volume %. LFL = Lower Flammability Limit, UFL = Upper Flammability Limit, DPL = Downward Propagation Limit, UPL = Upward Propagation Limit

Fuel	LFL		UFL	Inert (N_2)
	UPL	DPL		
H_2	3	6	84	~60
CH_4	5		50	70

Table 2: Flammability limits for fuel-N_2O mixtures at NTP. Amounts are given in volume %.

A standard approach to calculate the pressure loads during combustion of these mixtures is to use constant volume explosion estimates (AICC- adiabatic, isochoric, complete combustion) based on chemical equilibrium ideas. For this purpose, the computer program STANJAN [2] which is based on the JANNAF thermochemistry data and minimization of Gibbs energy was used in this study. Although this approach is reasonably reliable, there are some cautions about using these values in safety assessments:

1. Incomplete combustion occurs near the lower flammability limit for H_2.
2. There are cellular instabilities and a strong Lewis number effect for H_2.
3. N_2O undergoes partial or no reaction in lean mixtures.
4. Ignition energies are very high for large amounts of N_2O and small amounts of fuel.

In general, it is found that the H_2 component dominates the behavior of mixtures. Estimates of peak pressure and temperature in fuel-air explosions are given in Fig. 1, and for fuel-nitrous oxide mixtures in Fig. 2. In this study, the nitrous oxide consumption close to the lower flammability limits of H_2-N_2O-air and CH_4-N_2O-air mixtures was investigated at an initial pressure of 100 kPa and an initial temperature of about 22^{o}C. In addition, we have measured flammability limits and ignition energy bounds of methane-nitrous oxide mixtures with nitrogen dilution.

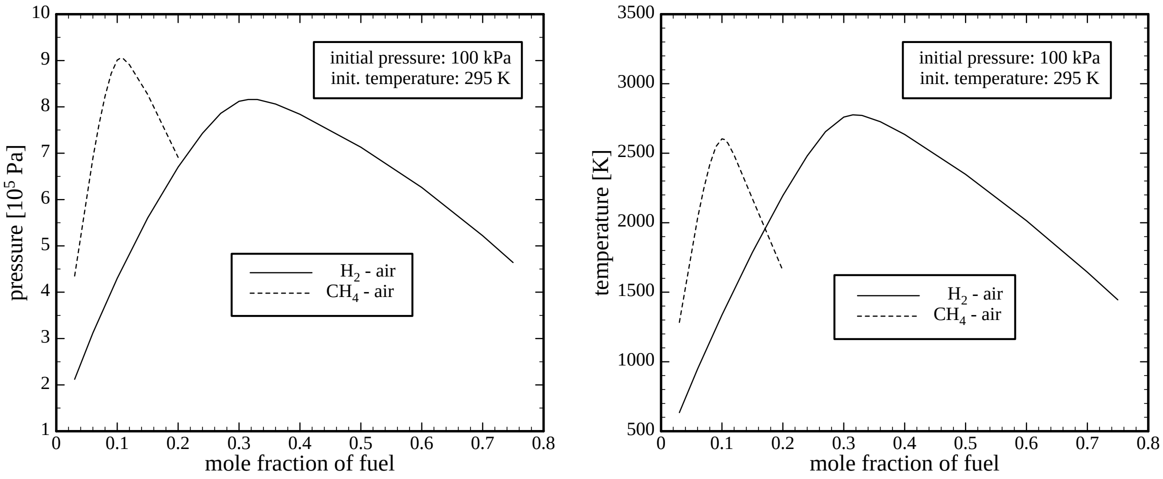

Figure 1: Constant volume explosion pressures and temperatures in fuel-air mixtures, initial conditions of 100 kPa and 295 K.

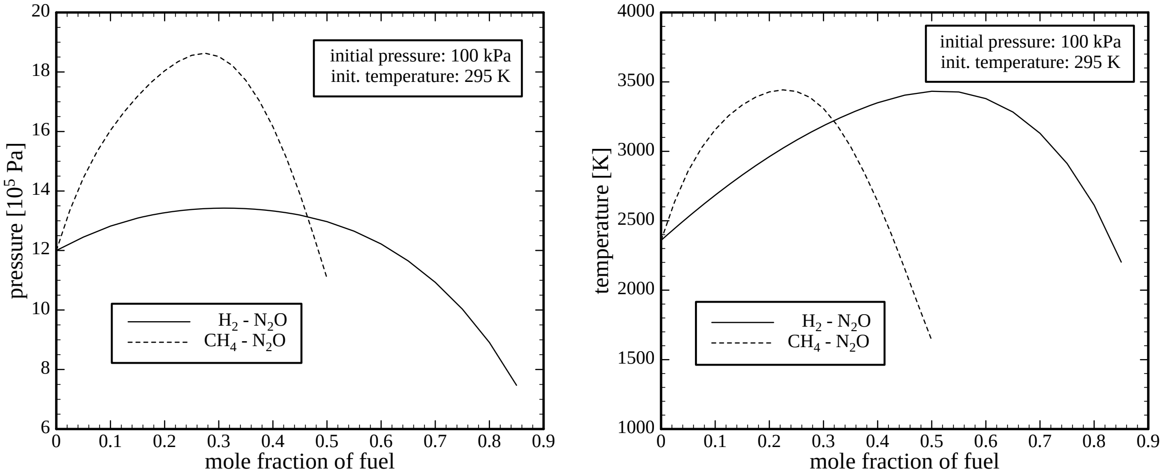

Figure 2: Constant volume explosion pressures and temperatures in fuel-N_2O mixtures, initial conditions of 100 kPa and 295 K.

2 Apparatus

The present experiments were done in a constant volume (11.25 liters) combustion vessel (CV in Fig. 3). The vessel was constructed of steel slabs and formed a rectangular chamber with internal dimensions of 190 mm × 203 mm × 305 mm. The vessel was filled with a mixture of gases using partial pressures to determine composition. The gas handling system is shown in Fig. 3. In order to reduce the potential for accidental explosion hazards, several safety features (check valves, gas detectors, logic valve control circuits), which are not shown in Fig. 3, were utilized. The products were exhausted through a treatment system following combustion, which is described in detail in [3].

The combustion facility was instrumented with pressure and temperature sensors. The static pressure gauge to meter the initial pressures of the reactants and the final pressure of the products was a digital pressure indicator (Heise, model 901A) with a range from 0 to 250 kPa absolute and an accuracy of ±0.18 kPa. A dynamic gauge (Kulite Semiconductor Pressure Gauge, model XTME-190-250A) was used to monitor the explosion pressure. This is a piezoresistive type transducer which has a combined nonlinearity, hysteresis and repeatability of 2.5 kPa. This transducer was protected by two porous metal frits, which are sufficient to shield the transducer from temperature but do not affect the pressure reading. A thermocouple (Omega, type K) with a 3.2 mm metal sheat was installed above the center of the spark source. Each wire was 24 AWG, and the weld bead size was approximately 1.5 mm. An electronic cold-junction (Omega, model DP462) and temperature readout was used to convert the thermocouple output to temperature. The pressure and temperature signals were recorded on a personal computer (Labview Data Acquisition Software). Furthermore, the vessel was equipped with 25-mm thick glass windows with a clear aperature of 117-mm diameter. Through

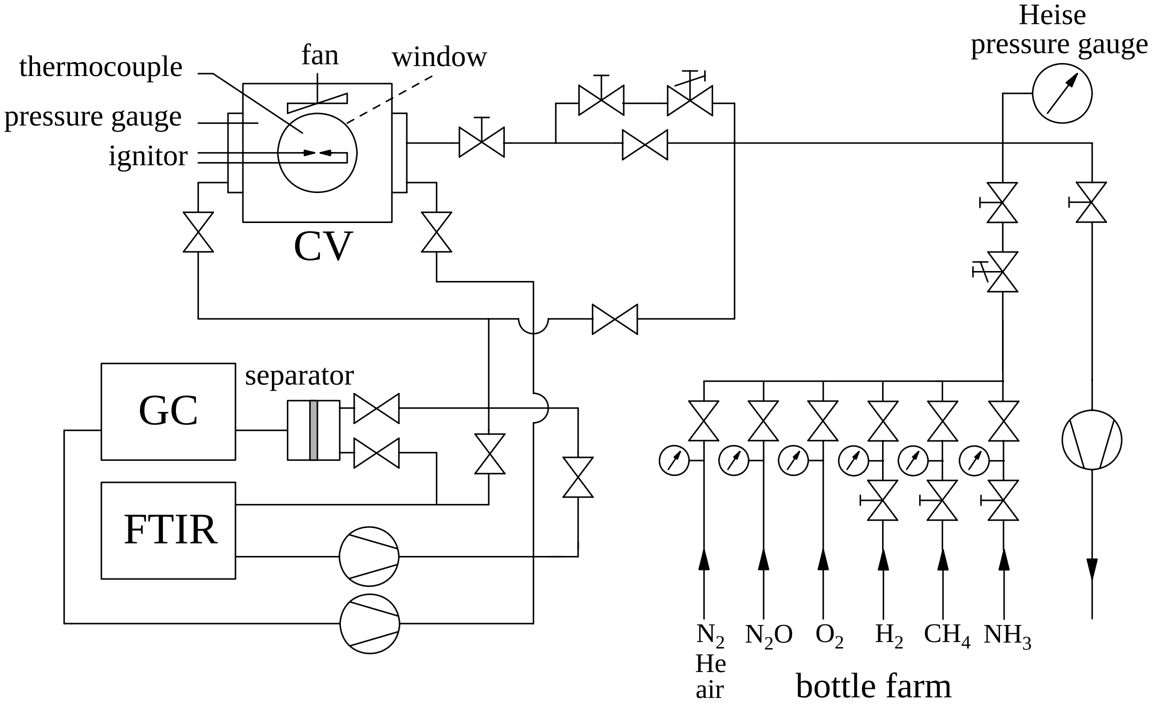

Figure 3: Schematic diagram of the constant volume combustion vessel, gas supply, vacuum system and the gas sampling facilities.

these windows, a color-schlieren video-system was used to observe the flame initiation and propagation. Figure 4 shows a schematic diagram of the optical set-up of the color-schlieren video-system.

An electric spark was used to initiate the flame. The spark gap (3-6 mm depending on the gas composition) was positioned in the center of the vessel and the electrodes passed through Teflon insulators on the sides of the vessel. The power for the spark was provided by a 0.5 μF capacitor charged by a Hipotronics 15 kV power supply. The discharge across the gap was triggered by a 30 kV pulse (low current) from an EG&G TM-11A power supply. Figure 5 shows a schematic diagram of the electrical circuit of the spark ignition system. The circuit was motivated by the design described in [4].

All investigations were carried out under turbulent gas conditions. The turbulence was produced by a single mixing fan with two blades, about 150 mm in diameter. The mixing fan was driven by a pulley drive (6.7:1 reduction) from a universal motor controlled by a speed control (light-dimmer switch). The shaft for the fan was connected to a magnetic torque transmitter which was located at the top of the vessel. Flow measurements were made[1] near the ignition location with a single-component laser doppler anemometer (LDA). The signals were processed (Dantec Counter, model 55L96) to obtain mean $\overline{u}$ and

---

[1] The authors thank Kumar Raman for carrying out these measurements.

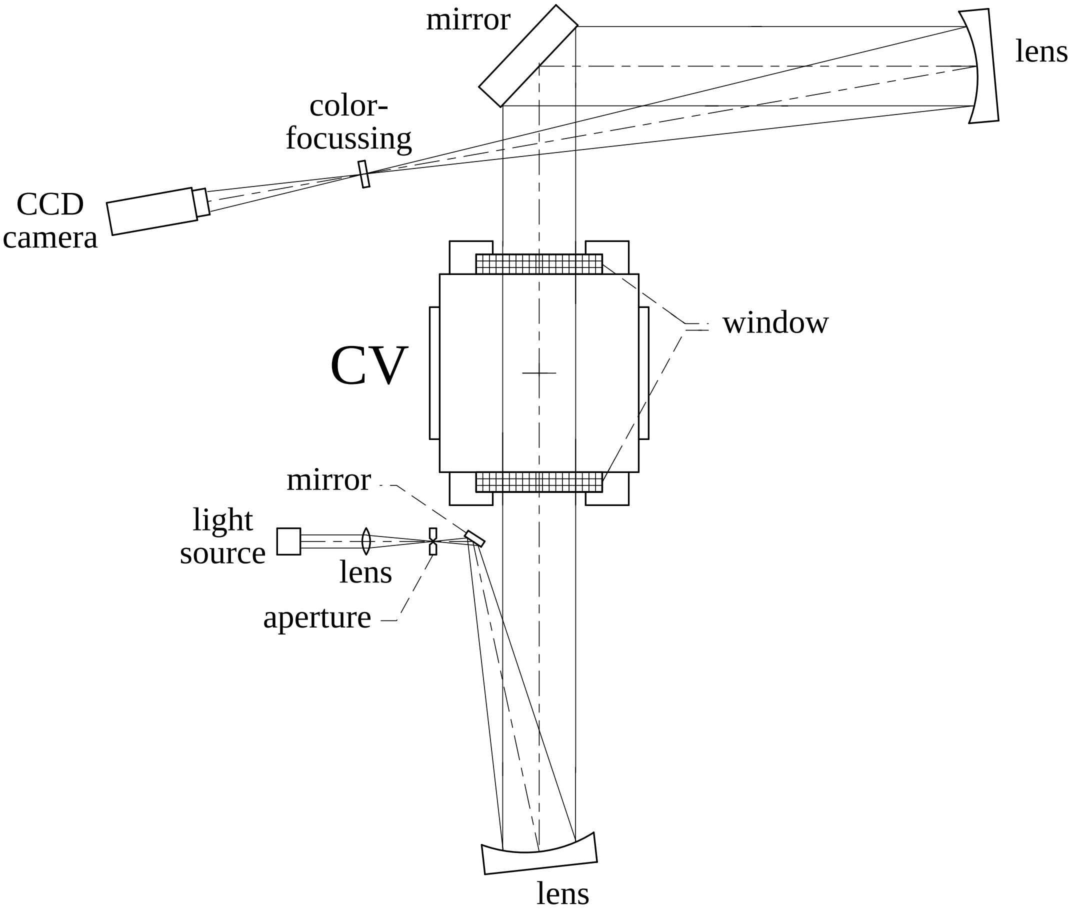

Figure 4: Schematic diagram of the color-schlieren video-system.

fluctuating velocities u_{rms} in the vertical direction. The results of these measurements are given in Table 3. Mean flow velocity and fluctuations increase with fan rotational speed, however the turbulence intensity $u_{rms}/\overline{u}$ was found to be relatively independent of the rotational speed. Measurements at various locations (results are not presented in Table 3) also indicate that the turbulence intensity is relatively independent of position.

Fan speed	$\overline{u}$ [m/s]	u_{rms} [m/s]	$u_{rms}/\overline{u}$
low	0.41	0.10	0.24
medium	0.65	0.17	0.26
high	0.85	0.22	0.26

Table 3: Initial vertical flow velocity and turbulence intensity in the center of the combustion vessel near the ignition location.

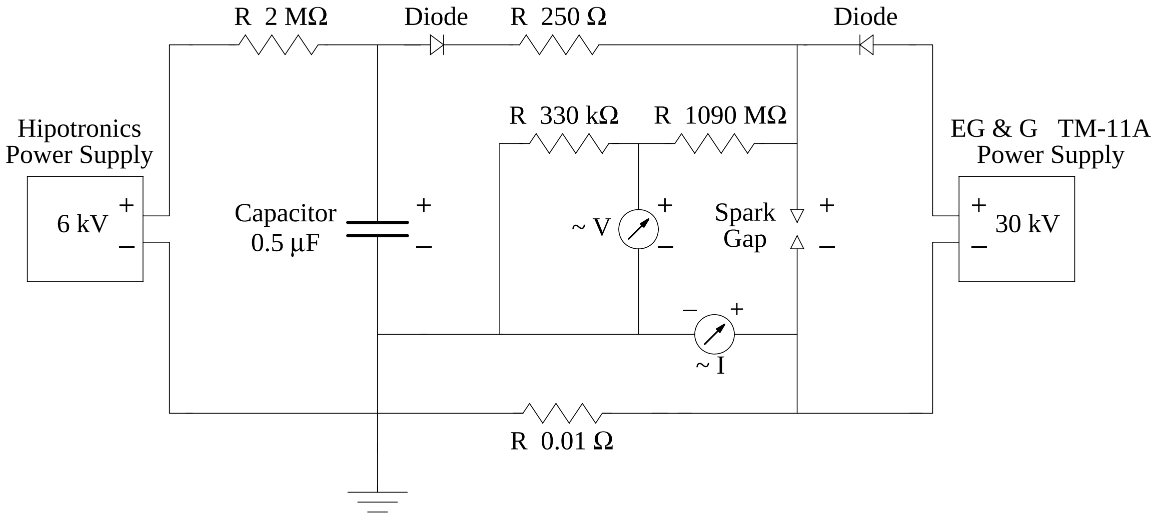

Figure 5: Schematic diagram of the spark ignition system.

3 Gas Analysis

The experimental studies reported subsequently were carried out using pre- and post-burn gas analysis. For these analysis, the vessel was connected with a gas chromatograph (GC) and a Fourier transform infrared spectrometer (FTIR) by a sampling loop (see GC and FTIR in Fig. 3). This loop could be evacuated and the test gas was pumped through the system to get a homogeneous mixture. The detected and quantified substances were the fuels H_2 and CH_4, the oxidizers N_2O and O_2, and also the inert component N_2.

The Gas Chromatograph (MTI Analytical Instruments M200) was equipped with two columns, column A: molecular sieve MS-5A 10m, column B: poraplot Q OV-1 4m, 2μm. The instrument was supplied by Westinghouse Hanford Company and set up by H.A. Frey and C.J. Hewitt of CST-6, Los Alamos National Laboratory.

Calibrations between measured area counts and the gas partial pressure, and also all gas analyse, were done at a total pressure of 100 kPa. In case the post-burn total pressure differs more than ± 2 kPa from 100 kPa (which is usually the case), the pressure was corrected by filling with nitrogen or by evacuation. The composition results were then corrected to compensate for this change in pressure in the vessel. This was found to be an important step in carrying out accurate measurements with the GC. Another important step in the procedure was to bake the molecular sieve column out at 180°C overnight before each set of measurements. Even though the inlet to the GC used a H_2O membrane separator (A+ corporation, Genie model 101), such large quantities of H_2O were produced in these experiments that the daily bake out was needed to remove H_2O from the molecular sieve column. Otherwise large shifts in the retention times and concentration-area relationships were observed. GC sampling times were also reduced to a minimum and the detectors operated at the lowest sensitivity to avoid saturation. The sample loop also had to be operated in a very consistent fashion in order to get consistent results. By carrying out all of these steps, excellent repeatability was obtained with the GC. As shown in Figs. 6 and 7, the resulting area-concentration relationships were very linear and repeatable.

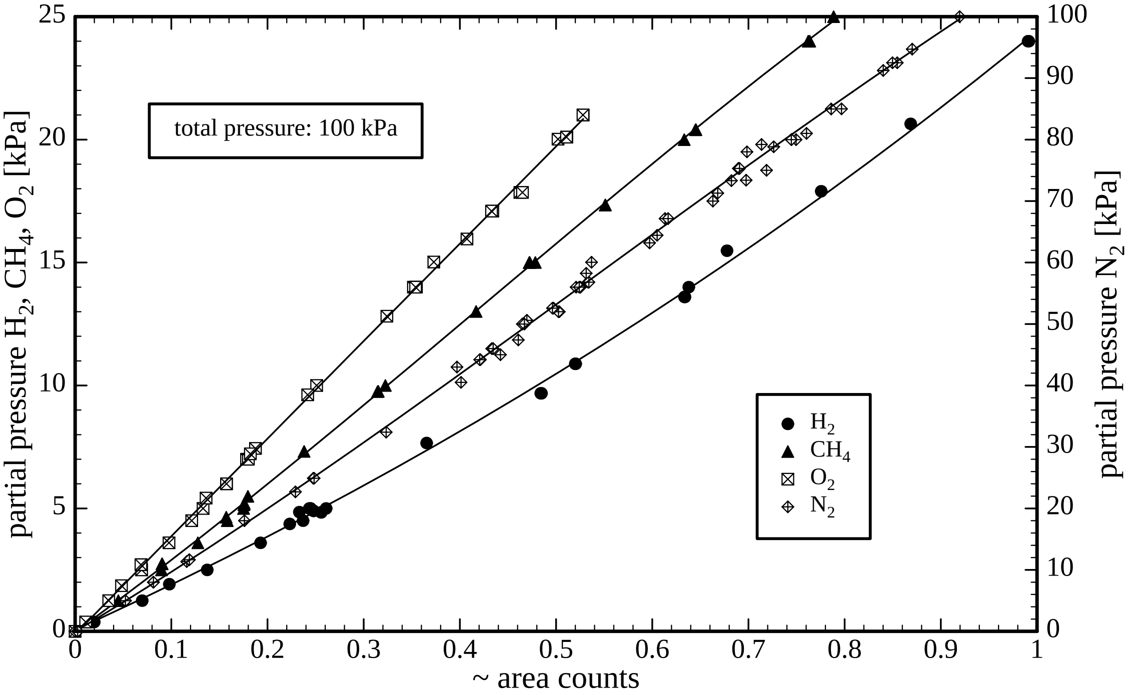

Figure 6: Gas chromatograph calibration for hydrogen, methane, oxygen and nitrogen.

The molecular sieve (column A) was used to quantify oxygen (0 - 20 kPa) and nitrogen (0 - 95 kPa). The retention times were about 54 s for oxygen and 87 s for nitrogen. The poraplot Q (column B) was used to quantify hydrogen (0 - 24 kPa), methane (0 - 24 kPa) and nitrous oxide (0 - 15 kPa). The retention times were about 22.5 s for hydrogen, 25.5 s for methane and 34 s for nitrous oxide. Figures 6 and 7 show the calibration between the area counts and the gas partial pressures.

The FTIR Spectrometer (MIDAC Corporation M2000) was used to quantify the gas partial pressure of nitrous oxide. The basic theory of operation of this spectrometer system is given by Beer's law. This law states that for parallel, monochromatic radiation that passes through an absorber of constant concentration, the transmittance of a stable solution is an exponential function of the concentration of the absorbing solute:

$$log\left(\frac{1}{T}\right) = A = \alpha \cdot b \cdot C \ , \tag{1}$$

where: T = transmittance, A = absorbance, α = absorptivity or extinction coefficient, b = optical path length and C = molar concentration of the absorbing species.

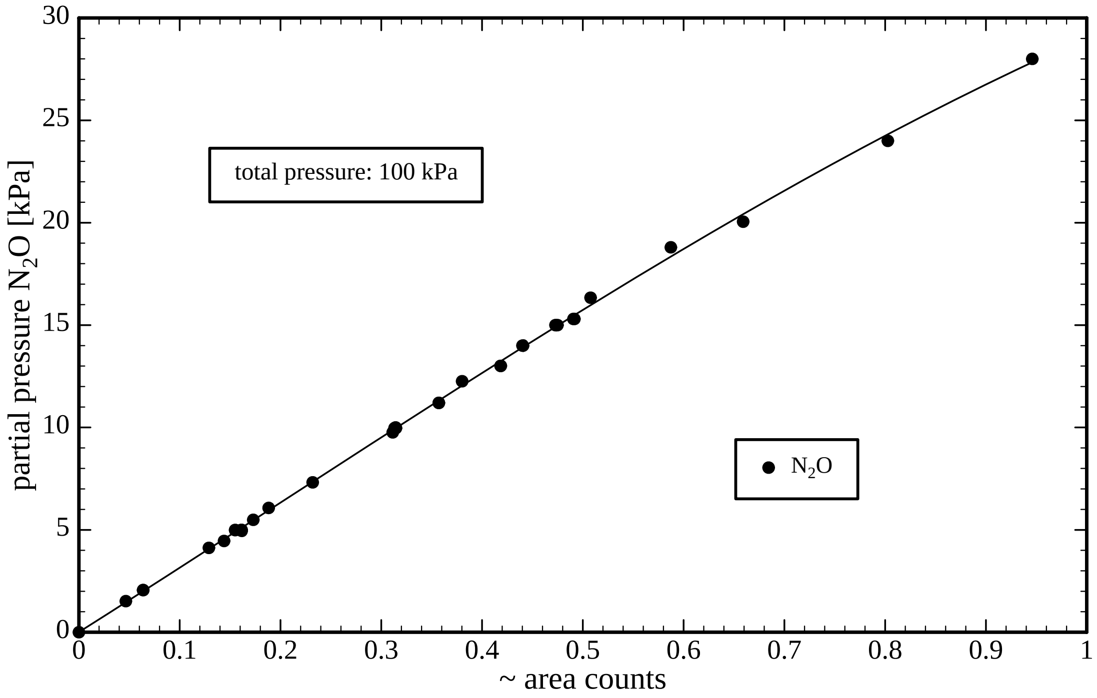

Figure 7: Gas chromatograph calibration for nitrous oxide.

The FTIR measures the transmittance T as a function of wavelength λ or wavenumber $1/\lambda$. A constant extinction coefficient $\alpha(\lambda)$ gives a linear relationship between concentration and absorbance for each absorbing species at a selected wavelength. However, the extinction coefficient is actually a function of the gas concentration so that a nonlinear relationship exists between concentration and absorbance. This relationship was determined by calibration tests in which the FTIR cell was filled by the method of partial pressures with known amounts of the test gases. The absorbance spectrum $A(\lambda)$ was then analyzed to determine the appropriate range of wavelengths for carrying out the calibration between absorbance and gas concentration (partial pressure). It was important to choose a spectral range that was not obscured by water vapor (always present in the spectrum) or other IR-active gases in the system. A spectral range with a low extinction coefficient was also desirable in order to obtain a large dynamic range. Many of the N_2O bands were so intense that the absorbance saturated at high concentration. For nitrous oxide, a very reliable calibration between gas partial pressure and absorbance could be found from 0 to 15 kPa at the wavenumber 3462.9 cm^{-1} (see Fig. 8).

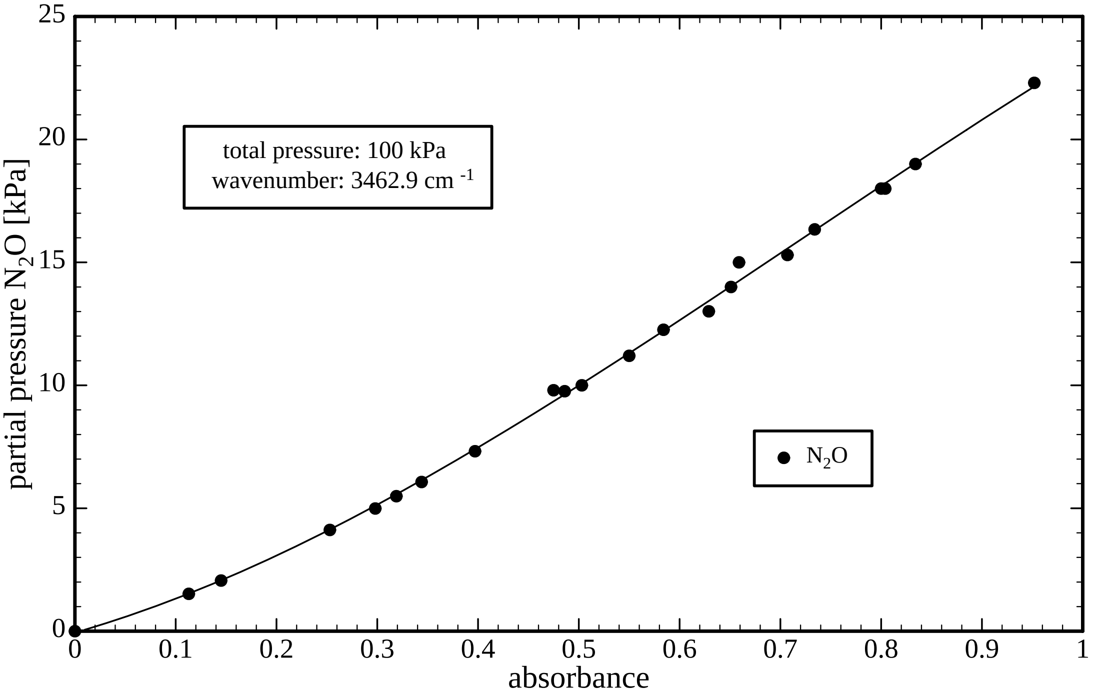

Figure 8: Fourier transform infrared spectrometry calibration for nitrous oxide.

4 Results and Discussion

4.1 Nitrous Oxide Consumption

By analyzing the pre- and post-burn gas composition, (see chapter *Gas Analysis*) the nitrous oxide consumption during combustion of fuel-nitrous oxide-air mixtures was measured. The mixtures investigated were hydrogen-nitrous oxide-air and methane-nitrous oxide-air. For all nitrous oxide consumption tests, the pre-burn total pressure was 100 kPa and the initial gas partial pressure of nitrous oxide was nominally 10 kPa.

Hydrogen-Nitrous Oxide-Air Mixtures

For these investigations, the initial gas partial pressure of hydrogen was varied from 5.7 to 13.9 kPa, whereas the initial partial pressure of nitrous oxide was nominally 10 kPa. Figure 9 shows five typical pressure histories for these tests. The peak pressure increases with increasing H_2 concentration: 2.4 bar (5.7 kPa H_2), 3.3 bar (7.5 kPa H_2), 4.0 bar (8.6 kPa H_2), 5.1 bar (10.2 kPa H_2), 6.5 bar (13.9 kPa H_2).

These results are very similar to what was obtained in earlier studies in a combustion vessel of 400 l capacity by Ross and Shepherd [3] and in a 120 l vessel by the Bureau of Mines [5] (see Fig. 10). There are some differences since the N_2O concentration is held

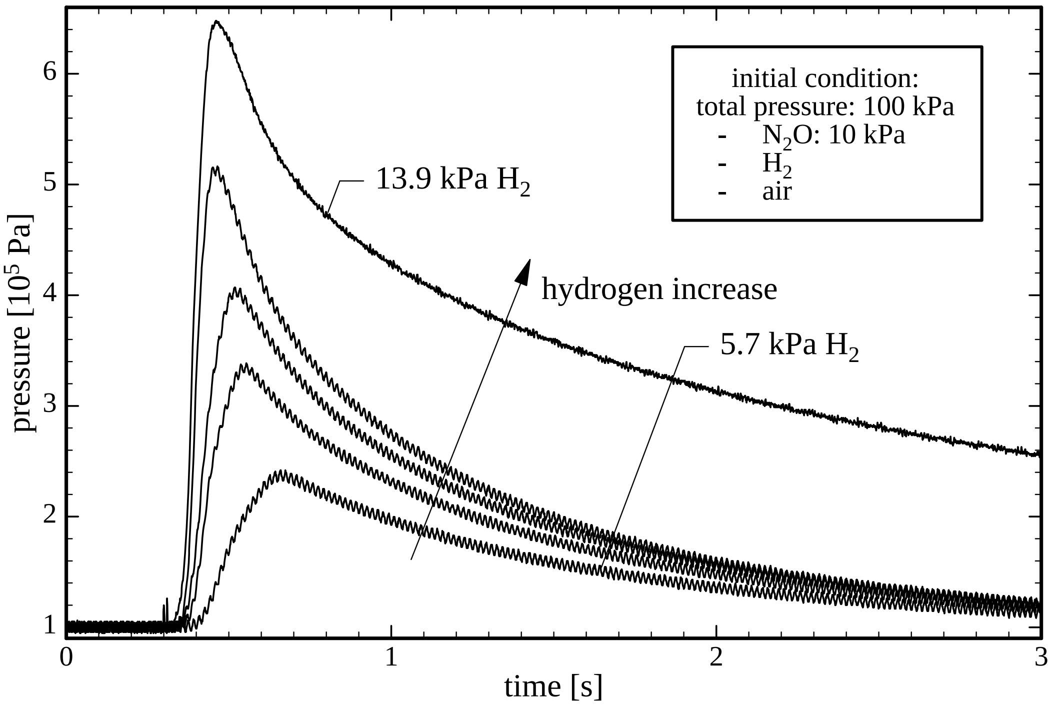

Figure 9: Combustion pressure histories of lean hydrogen-nitrous oxide-air mixtures.

fixed in the present experiments and was variable (proportional to the H_2 concentration) in the Bureau of Mines experiments. However, the values for turbulent conditions appear to define a clear upper bound to the peak pressure that is a continuous function of H_2 concentration down to 4%. The quiescent values show the characteristic sharp cutoff at 8% hydrogen corresponding to the downward propagation limit.

Figure 11 shows the results of the nitrous oxide consumption during hydrogen-nitrous oxide-air mixture combustion. At 5.7 kPa initial H_2 almost no nitrous oxide is consumed. The final nitrous oxide amounts to 9.15 kPa and the final pressure of hydrogen amounts to 1.4 kPa. With an increasing amount of initial hydrogen the final amount of hydrogen varies between 0.2 and 0.6 kPa, whereas the final amount of nitrous oxide decreases. Above 10 kPa initial hydrogen, the final nitrous oxide amount is below 1 kPa and at 13.9 kPa initial hydrogen the nitrous oxide is almost completely consumed (0.15 kPa).

The results shown in Fig. 11 are the first quantification of the N_2O participation effects. These effects were noted by Cashdollar et al. [5] but they were unable to make quantitative measurements due to problems with their gas sampling system. Ross and Shepherd [3] were not equipped to do gas sampling and examined variations in final pressure to attempt to determine the participation limit for H_2–N_2O–NH_3 mixtures. A value of 13% fuel was estimated for the critical amount needed to fully react the N_2O. The present results indicate that a value of 10% is more appropriate when the fuel is H_2, and as discussed subsequently, as little as 5% is required when the fuel is CH_4.

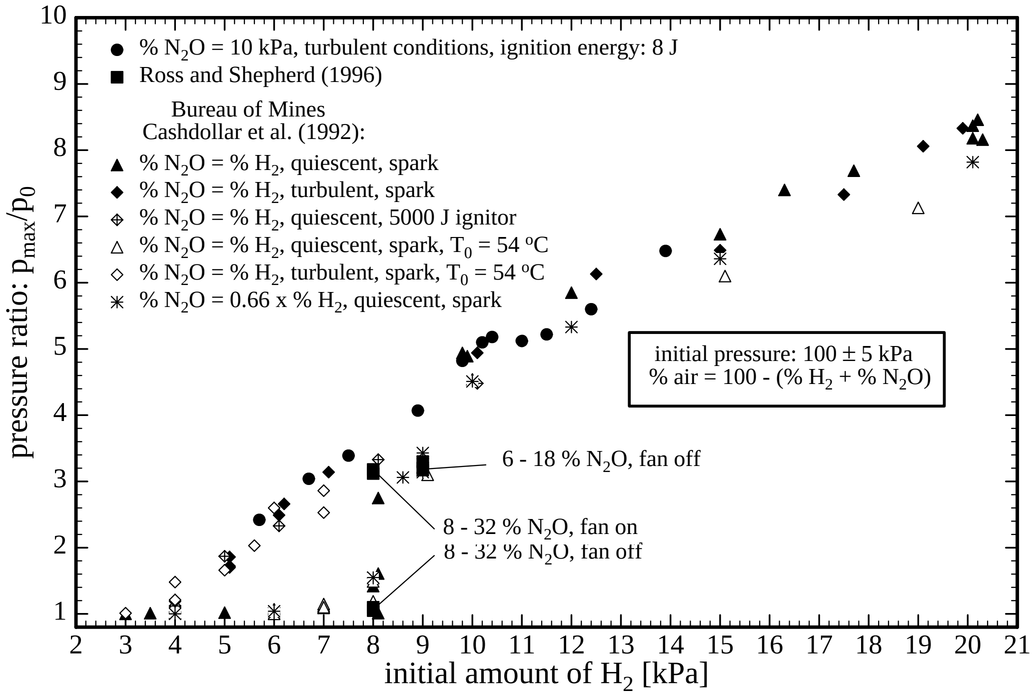

Figure 10: Peak combustion pressure in lean hydrogen-nitrous oxide-air mixture combustion.

Final Pressure Evaluation

The measured final pressure in the vessel after the combustion and cooling of the products to room temperature provides additional information about the combustion process. This value (compared to calculations) has been used in previous studies to get some insight into the possible set of product compositions.

Figure 12 shows comparisons between measured (actual) and calculated final pressures (STANJAN [2]) for hydrogen-nitrous oxide-air and hydrogen-air mixtures. Adiabatic combustion at constant volume is used to define an ideal explosion pressure, temperature and product composition. A constant-volume cooling process with condensation of water was then assumed in order to compute the final pressure. The nitrous oxide in the reactants was divided into a reacting and an inert part corresponding to the nitrous oxide consumption measured in the experiments. All gaseous products were taken into account in these calculations. The partial pressure of water was fixed at 2.5 kPa corresponding to the saturation pressure of water at 21°C.

The difference between actual and STANJAN values may be caused by either condensed components which are not taken into account by the STANJAN calculations or systematic errors in measurement of temperature and correction for water vapor. A comparison between the two different mixtures (with and without N_2O) shows similar

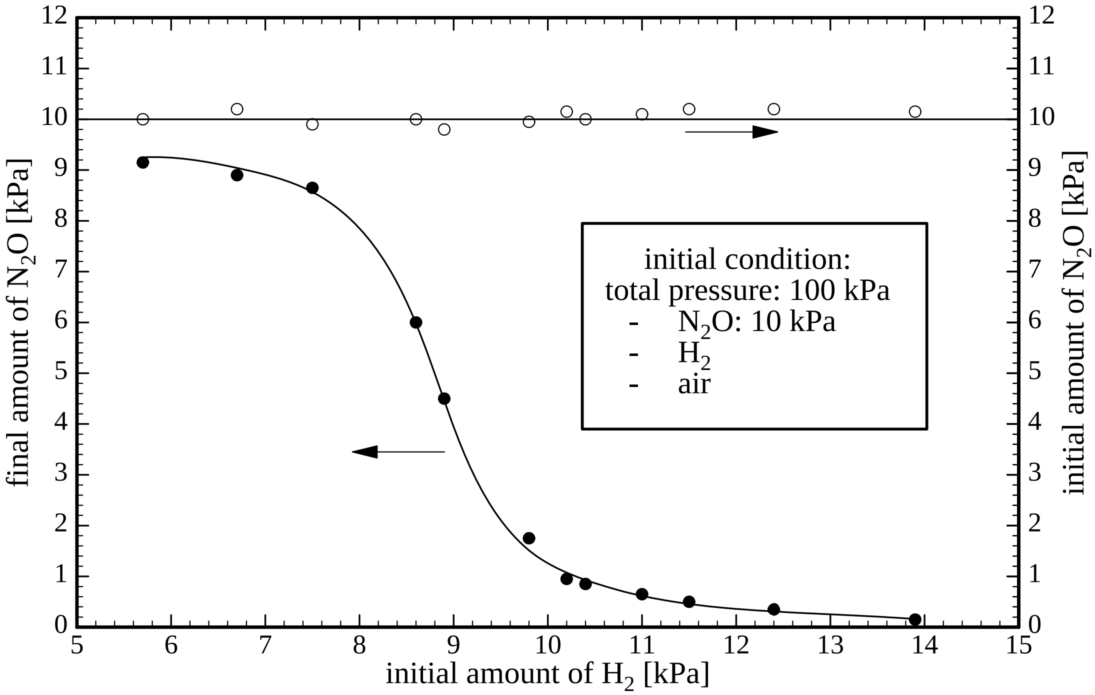

Figure 11: Nitrous oxide consumption in lean hydrogen-nitrous oxide-air combustion.

differences between actual and calculated final pressure. This indicates that the putative liquid compounds do not contain significant amounts of nitrogen, making this an unlikely explanation. More probable is that the vessel temperature is nonuniform and not equal to the thermocouple temperature. This creates an uncertainty in the fraction of water condensed which will propagate as a systematic error in the estimated final pressure. Much greater care in the vessel temperature control and more detailed measurements of the gas and wall temperatures would be needed to improve the accuracy of the final pressure technique. The present gas sampling system is an effective solution to the composition measurement issue that avoids this additional complexity.

Methane-Nitrous Oxide-Air Mixtures

For these investigations, the initial gas partial pressure of methane was varied from 4.5 to 10.0 kPa, and the initial partial pressure of nitrous oxide was nominally 10 kPa. Figure 13 shows the pressure histories for these tests, in which the pressure peak increases with increasing CH_4 concentration from 5.9 bar (4.8 kPa CH_4) over 6.1 bar (4.9 kPa CH_4) and 8.1 bar (7.9 kPa CH_4) to 9.2 bar (10.0 kPa CH_4). The pressure history for 5.9 kPA CH_4 is atypical and should not be used in analysis.

Figure 14 shows the results of the nitrous oxide consumption during methane-nitrous oxide-air mixture combustion. The results are very different from the results of hydrogen-

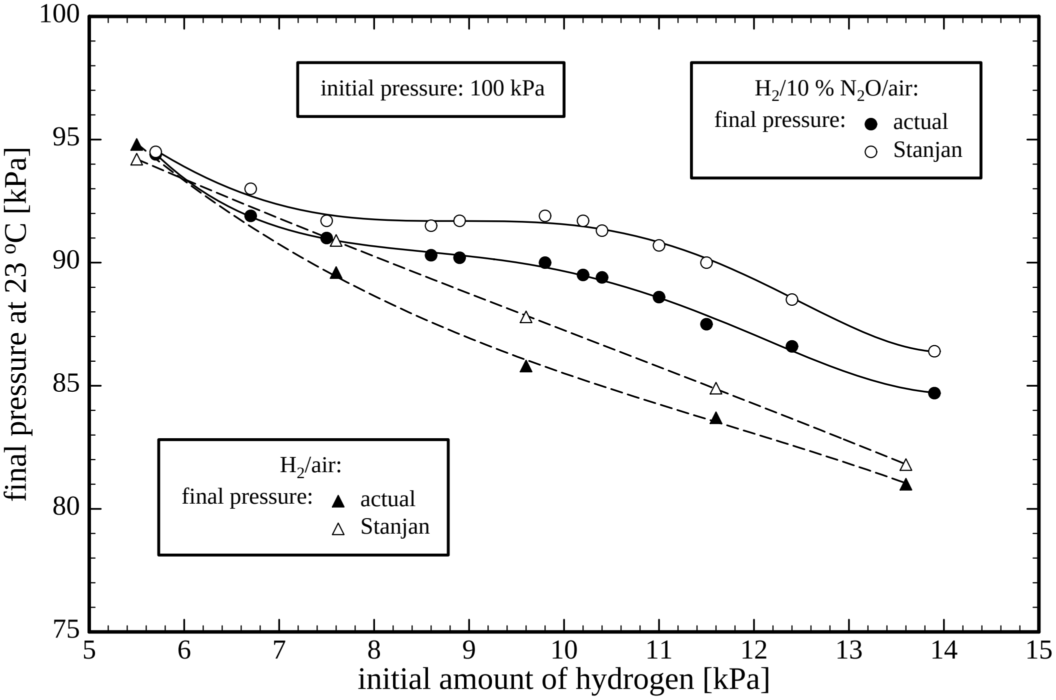

Figure 12: Final pressure. Comparison between post-burn measurements and STANJAN calculations.

nitrous oxide-air mixtures presented above. If the mixture is flammable, the nitrous oxide is almost totally consumed. For initial methane amounts above 4.8 kPa the final amount of nitrous oxide varies between 0.25 and 0.35 kPa and the final amount of methane is below 0.4 kPa. For 4.5 kPa initial methane, the mixture is not flammable and therefore no methane or nitrous oxide is consumed. Compared to H_2–N_2O–air mixtures the heat of combustion of CH_4–N_2O–air mixtures is higher. Therefore, the flame temperature at the flammability limit will be much higher for CH_4 than in the case of H_2. It follows that the rate of thermal decomposition of N_2O

$$N_2O + \ (M) \ \rightarrow \ N_2 + \ O \ + \ (M)$$

with an Arrhenius activation energy of around 60 kcal/mole [6] will be sufficiently high at the CH_4 LFL and decomposition will always occur.

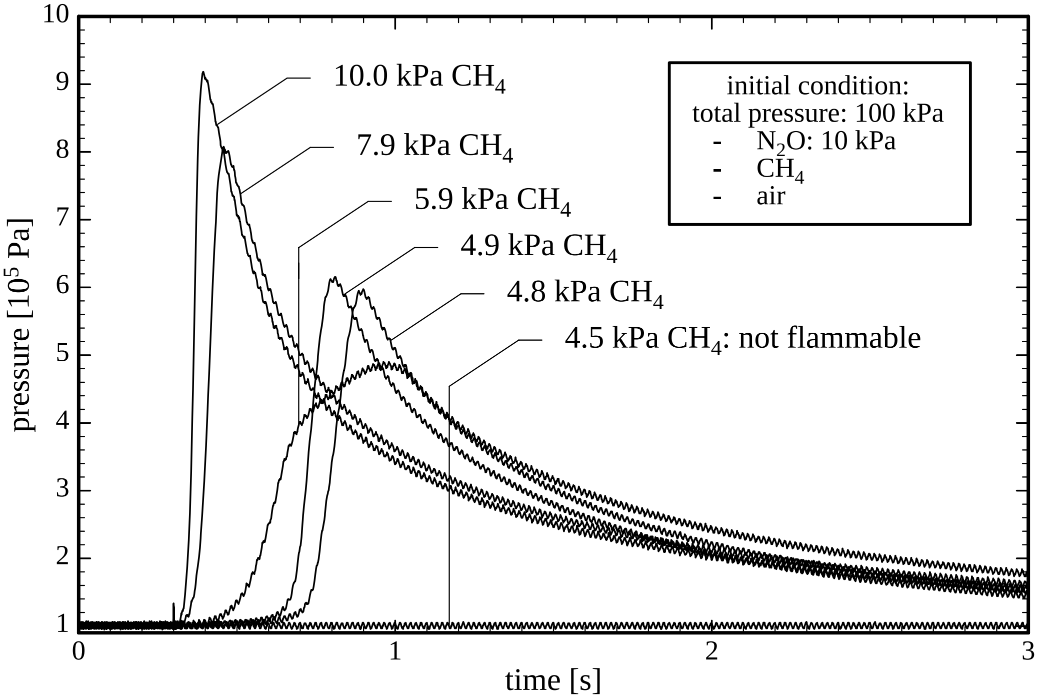

Figure 13: Combustion pressure histories of methane-nitrous oxide-air mixtures.

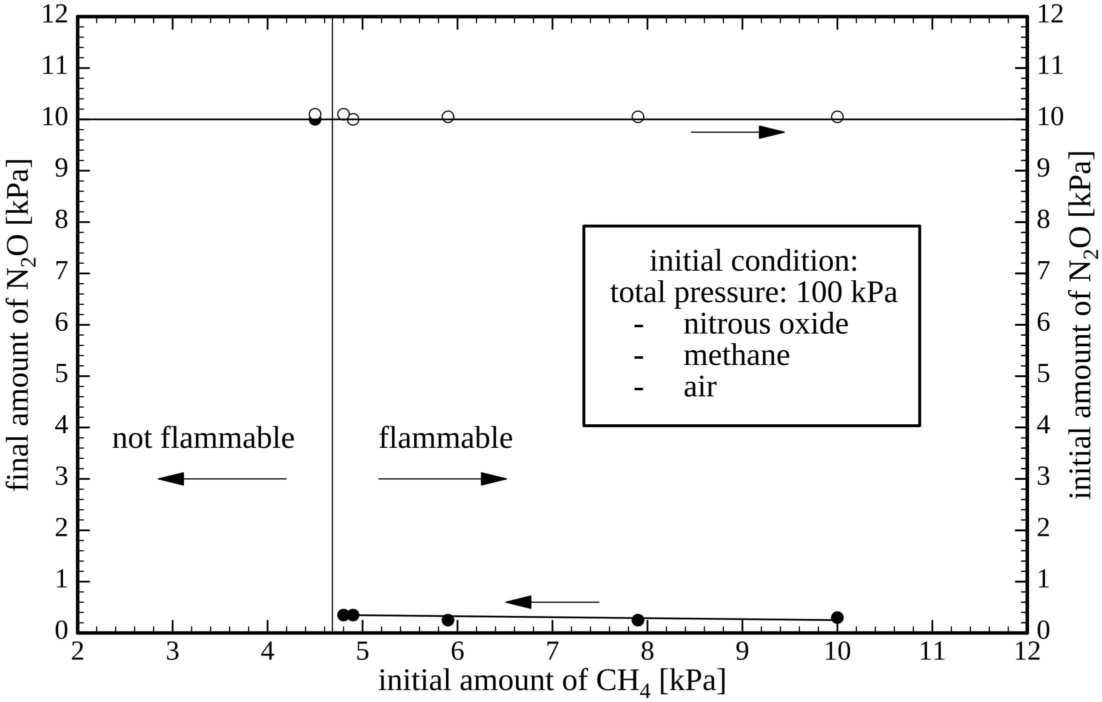

Figure 14: Nitrous oxide consumption in methane-nitrous oxide-air combustion.

4.2 Flammability Limit

Hydrogen-Nitrous Oxide-Nitrogen Mixtures

Numerous flammability studies have been conducted with hydrogen. Some of these studies have been carried out with N_2O as the oxidizer [7, 8, 9, 10]. The available data are shown in Fig. 15 together with the flammability limits of hydrogen-oxygen [11] and hydrogen-air-nitrogen mixtures [12, 13]. These data are all nominally obtained at 25°C and 1 atm pressure. Not shown on this diagram are the H_2–N_2O–air mixture data of [3] and [5]. Note that the rich limit data of Posthumus are substantially below those of Smith and Linnett. This is apparently due to the low temperature/energy ignition source of Posthumus in comparison to the 20 J spark discharge used by Smith and Linnett. In general, ignition energy has a strong effect on flammability limits in mixtures containing large amounts of N_2O.

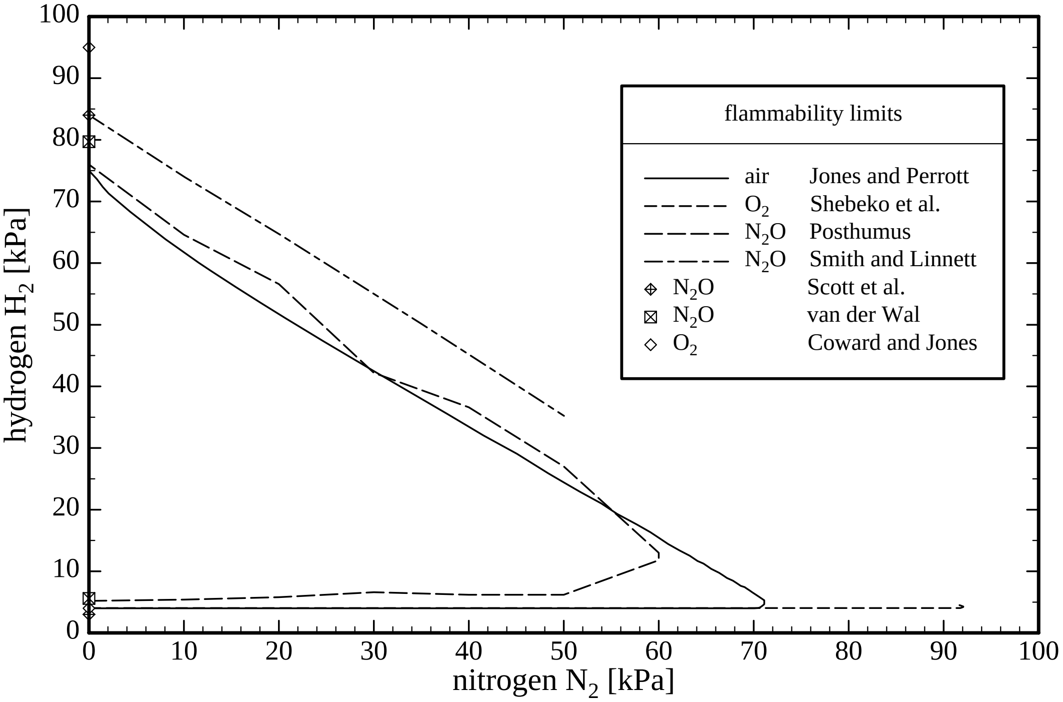

Figure 15: Flammability limits of hydrogen-air-nitrogen, hydrogen-nitrous oxide-nitrogen and hydrogen-oxygen-nitrogen mixtures.

Methane-Nitrous Oxide-Nitrogen Mixtures

Measurements with methane-nitrous oxide-nitrogen mixtures were carried out to determine flammability limits and ignition energy bounds. Additional tests with methane-nitrous oxide-oxygen-nitrogen mixtures were done to investigate the influence of small amounts of oxygen on the flammability limit.

Flammability limits were determined for CH_4–N_2O–N_2 mixtures at a total initial pressure of 100 kPa. The ignition source was the capacitor discharge unit described in Fig. 5, which has a maximum electrical energy of around 8 J.

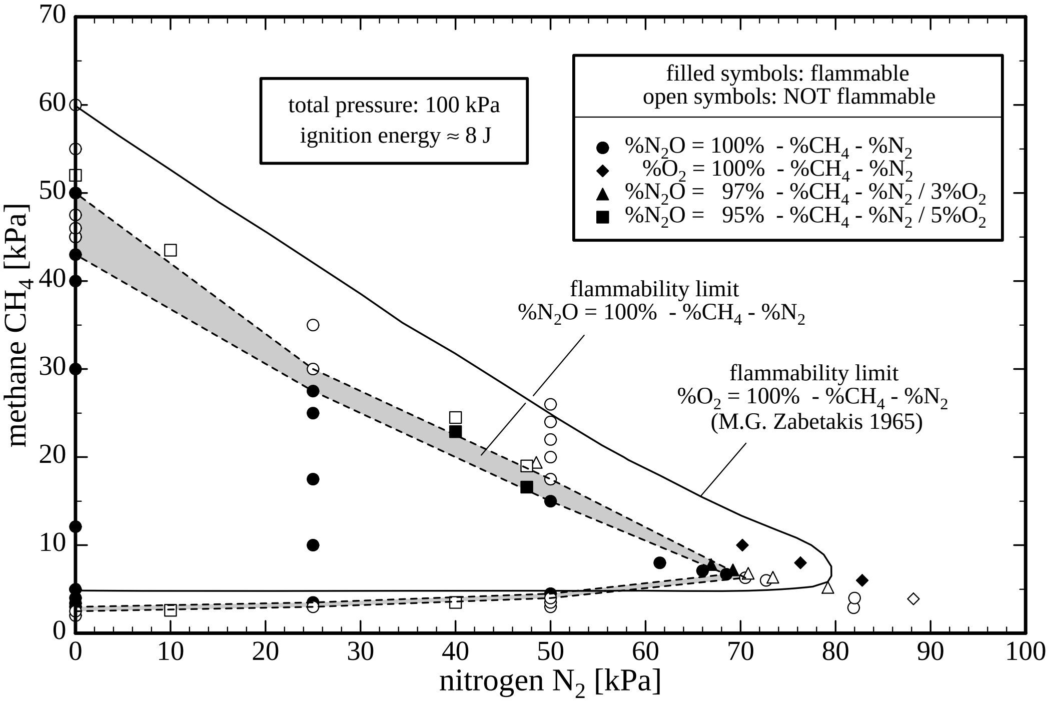

Figure 16: Flammability limits of methane-nitrous oxide-nitrogen, methane-oxygen-nitrogen and methane-nitrous oxide-oxygen-nitrogen mixtures.

The present results are shown in Fig. 16 and compared to previous results from the literature [12] for CH_4–O_2–N_2 mixtures. Previous results for CH_4–N_2O or CH_4–N_2O–N_2 mixtures were not available from the literature. The lower flammability limit shows a very smooth dependence (increase) on the amount of nitrogen dilution and a good correspondence to Zabetakis' results for CH_4–O_2–N_2, whereas the upper limit shifts to a smaller flammability region compared to CH_4–O_2–N_2 and shows a strong decrease with increasing nitrogen dilution. Without dilution, methane-nitrous oxide mixtures are flammable for methane partial pressures between 2.7 and 43-50 kPa. Mixtures with nitrogen dilution above 70.5 kPa are not flammable (inert). The corresponding methane partial pressure is 6.3 kPa.

Influence of Small Amounts of Oxygen (3 - 5%) on the Flammability Limit

Figures 16 and 17 show no pronounced dependence of the flammability limits of methane-nitrous oxide-nitrogen mixtures on small amounts of oxygen. At 3 kPa oxygen addition, the maximum flammable nitrogen dilution does not shift (see Fig. 17). Substituting oxygen for nitrous oxide shifts the maximum flammable nitrogen dilution (inerting concentration) from 70.5 to about 85 kPa (5 kPa CH_4 and 10 kPa O_2). Zabetakis obtained 80 kPa nitrogen dilution as the inerting concentration for CH_4–O_2–N_2 mixtures at atmospheric pressure and 26°C [12]. The present results exceed this value due to turbulent conditions (the mixing fan was on during the burn). Addition of 5 kPa oxygen at 0, 10, 40 and 47.5 kPa nitrogen dilution does not appreciably alter the flammability limit (see Fig. 16).

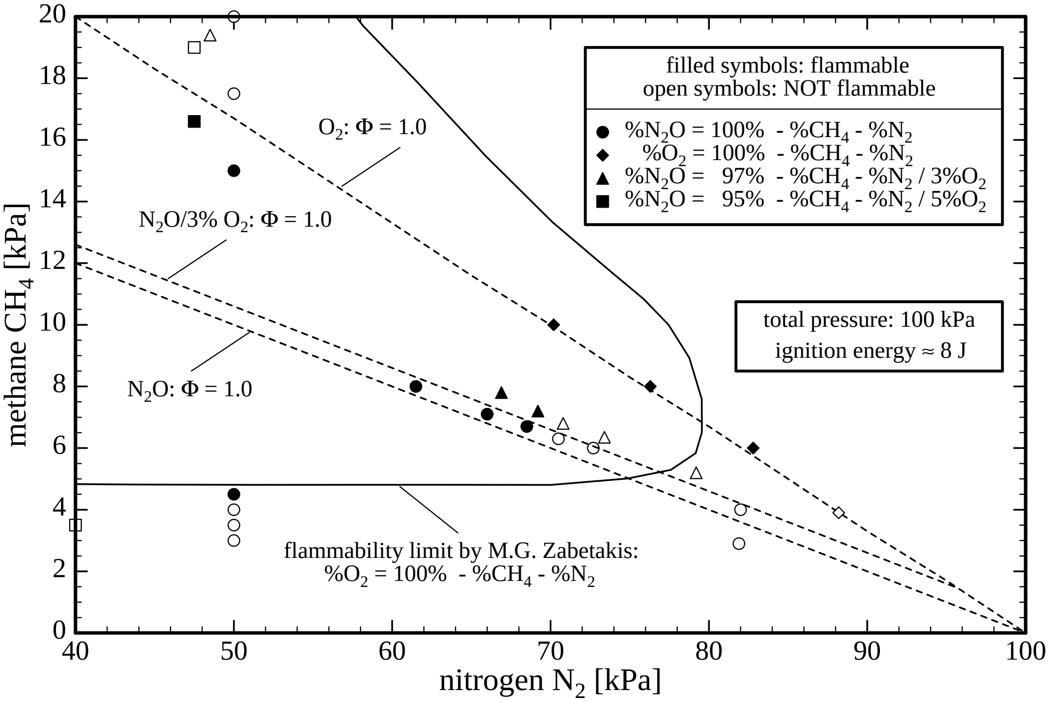

Figure 17: Influence of small amounts of oxygen on the flammability limit of methane-nitrous oxide-nitrogen mixtures.

Influence of Ignition Energy on the Flammability Limit

It is known [14] that the minimum ignition energy is a strong function of composition near the flammability limit. The minimum value of ignition energy for hydrocarbon fuels in air occurs for rich mixtures and is typically on the order of 0.25 mJ. Near the limits, a steep rise in minimum ignition energy is observed, with mixtures outside the flammability limit exhibiting inert behavior even for very large amounts of energy.

We determined bounds on the ignition energy by carrying out a series of tests with ignition energies of 0.04, 0.2, 1.0, 2.0, 5.0 and 8.0 J. For each ignition energy, the minimum amount of methane for flammability of a methane-nitrous oxide mixture at 100 kPa (no nitrogen dilution) was determined.

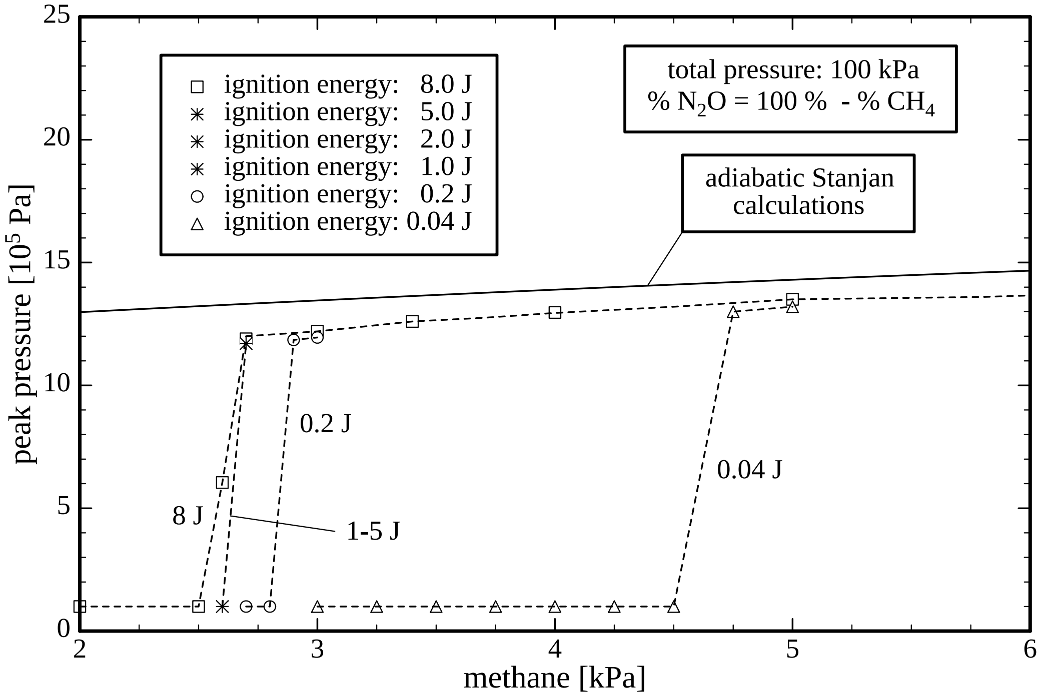

Figure 18: Peak pressure vs. methane concentration for various ignition energies.

The results of these runs are plotted in Figs. 18 and 19. Figure 18 shows the peak pressures compared to peak pressures resulting from STANJAN calculations. At the leanest flammable concentration (2.7% CH_4), the peak pressure is about 12 bar, close to the value obtained from N_2O decomposition alone (11.8 bar). This behavior is similar to that observed for H_2–N_2O mixtures by Cashdollar et al. [5], who found that with sufficient ignitor energy (5000 J), mixtures with as little as 1% H_2 could be ignited. Their limiting fuel concentration with a 58 J spark was about 6% H_2 for downward propagation. Hertzberg and Zlochower [15] propose that H-atoms catalyze N_2O decomposition and compounds such as H_2, CH_4 and NH_3 will, in small amounts (1-2%), accelerate the decomposition reaction sufficiently to stabilize the propagation of a decomposition flame. Substantial N_2O decomposition and associated high pressures have been observed for H_2, CH_4 and NH_3, the last being discussed by Jones and Kerr [16]. Note that the peak pressures are close to the 12 bar value that results from N_2O decomposition. These values seemed high to previous investigators who were used to modest pressures for near-limit combustion of hydrocarbon-air mixtures. It was common practice (and still is) to investigate flammability limits in hydrocarbon-air mixtures with a glass apparatus. The destruction of these experiments when investigating N_2O alarmed these investigators but

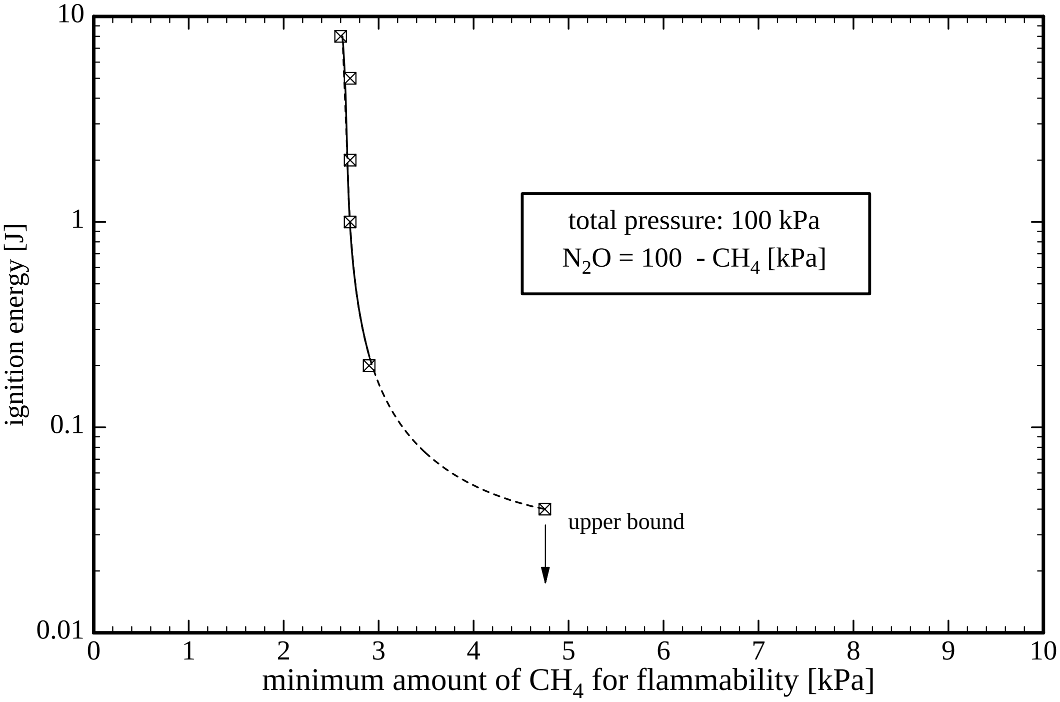

Figure 19: Minimum ignition energy as a function of methane concentration.

in hindsight it is a natural consequence of working with large amounts of N_2O.

Figure 19 shows the minimum ignition energy as a function of methane concentration near the flammability limit. These results show that for ignition energies above about 1.0 J, the flammability limit is independent of the ignition energy. Increasing the ignition energy from 40 mJ to 8 J reduces the ignition limit from 2.8 to 4.8% CH_4. Similar reductions in the LFL of H_2 have been obtained [5] in H_2–N_2O–air mixtures. However, experiments [5] using pyrotechnic ignitors and H_2–N_2O mixtures have shown that if the ignitor energy content is increased by several orders of magnitude (up to 5,000-10,000 J), then decomposition flames can be produced even [15] in the absence of any fuel!

We propose that the behavior of lean fuel–N_2O mixtures can be divided into two regimes: 1) low-to-moderate ignition energy (up to 100 J); 2) high ignition energy (above 5000 J). For the low-to-moderate energy regime, there is a well-defined minimum concentration of fuel (LFL) independent of ignition energy up to some value, at least 100 J. For the high-energy regime, decomposition reactions can be initiated irrespective of the amount of fuel as long as the energy is released rapidly enough. The precise details of the chemical and physical mechanism are not well understood at present but for the purposes of most safety assessments, it is probably sufficient to characterize the behavior in the low-to-moderate energy regime. It remains an intriguing problem in combustion science to determine the details of the flame initiation and propagation in very lean fuel–N_2O mixtures.

5 Conclusions

This study has provided significant new data on different combustion problems. The nitrous oxide consumption during combustion of hydrogen-nitrous oxide-air and methane-nitrous oxide-air (10 volume % N_2O) was investigated experimentally. Furthermore, the behavior of methane-nitrous oxide-nitrogen mixtures has been studied in detail. Lower and upper flammability limits have been determined. The influence of nitrogen dilution up to the inerting concentration, of small amounts of oxygen and of variation of the ignition energy on the flammability limits has been investigated in this study as well.

The behavior of nitrous oxide consumption in hydrogen-nitrous oxide-air mixtures is very different than in methane-nitrous oxide-air mixtures. Whereas the nitrous oxide completely dissociates during combustion of all flammable methane-nitrous oxide-air mixtures it only partially dissociates for lean hydrogen-nitrous oxide-air mixtures. For barely flammable hydrogen-nitrous oxide-air mixtures, almost no nitrous oxide is consumed.

The lower flammability limit of methane-nitrous oxide mixtures occurs at 2.7% methane for ignition energies less than 10 Joules. This value increases to 4.7% for ignition energies less than 0.04 Joule. The upper flammability limit is between 40 and 50% methane for ignition energies less than 10 Joules. Addition of 70% N_2 will inert the mixture. Small amounts of oxygen (3 - 5%) do not significantly influence the limits or inerting condition.

Acknowledgments

This work was supported by Los Alamos National Laboratory under Contract 929Q0015-3A, DOE W-7405-ENG-36.

References

[1] C. J. Danby and C. N. Hinshelwood. *Journal of Chemical Society*, page 464, 1940.

[2] W. C. Reynolds. *The Element Potential Method for Chemical Equilibrium Analysis: Implementation in the Interactive Program STANJAN.* Stanford University, Dept. of Mechanical Engineering, Stanford, CA, 3rd edition, January 1986.

[3] M. C. Ross and J. E. Shepherd. Lean combustion characteristics of hydrogen-nitrous oxide-ammonia mixtures in air. part i. Explosion Dynamics Lab Report FM96-4, California Institute of Technology, Pasadena, CA, July 1996.

[4] P. D. Ronney. Effect of gravity on laminar premixed gas combustion ii: ignition and extinction phenomena. *Combustion and Flame*, 62:121–133, 1985.

[5] K.L. Cashdollar, M. Hertzberg, I.A. Zlochower, C.E. Lucci, G. M. Green, and R. A. Thomas. Laboratory flammability studies of mixtures of hydrogen, nitrous oxide, and air. Final Report WHC-SD-WM-ES-219, Bureau of Mines, June 1992.

[6] W. D. Breshears. Falloff behavior in the thermal dissociation rate of N_2O. *Journal of Physical Chemistry*, 99:12529 – 12535, 1995.

[7] S. Smith and J. W. Linnett. The upper limits of inflammability of hydrogen–air and hydrogen–nitrous oxide mixtures. *J. Chem. Soc. (London)*, Part I:37–43, 1953.

[8] K. Posthumus. On explosion regions of gas mixtures, in which one or two of the gases are endothermic. *Rec. trav. chim.*, 49:309–347, 1930.

[9] M. J. van der Wal. Explosive and nonexplosive reactions between nitrogen oxides and flammable gases. *Rec. trav. chim.*, 53:97–117, 1934.

[10] F. E. Scott, R. W. Van Dolah, and M. G. Zabetakis. The flammability characteristics of the system H_2–no–N_2O–air. In *Sixth Symp. (Intl) Combustion*, pages 540–545, Pittsburgh, PA, 1957. The Combustion Institute.

[11] H. F. Coward and G. W. Jones. Limits of flammability of gases and vapors. Bulletin 503, Bureau of Mines, 1952.

[12] M. G. Zabetakis. Flammability characteristics of combustible gases and vapors. Bulletin 627, Bureau of Mines, 1965.

[13] Yu. N. Shebeko, S. G. Tsarichenko, A. Ya. Korolchenko, A. V. Trunev, V. Yu. Navzenya, S. N. Papkov, and A. A. Zaitzev. Burning velocities and flammability limits of gaseous mixtures at elevated temperatures and pressures. *Combustion and Flame*, 102:427–437, 1995.

[14] J.M. Kuchta. Investigation of fire and explosion accidents in the chemical, mining, and fuel-related industries—a manual. Bulletin 680, U.S. Bureau of Mines, 1985.

[15] M. Hertzberg and I.A. Zlochower. Explosibility of nitrous oxide gas: The effect of H-atom-bearing impurities. Abstract, Joint Meeting of British and German Sections of the Combustion Institute, March 29-April 3, Cambridge, England, 1993.

[16] E. Jones and J.C. Kerr. Inflammability limits of ammonia, nitrous oxide, and air. *J.S.C.I.*, 68:31–34, 1949.